

Numerical Simulation of Flame Acceleration and Fast Deflagrations Using Artificial Thickening Flame Approach

Sobhan Emami¹, Kiumars Mazaheri¹, Ali Shamooni¹, Yasser Mahmoudi²

¹ Faculty of Mechanical Engineering, Tarbiat Modares University
Tehran, Iran

² Department of Engineering, University of Cambridge
Cambridge, CB2 1PZ, United Kingdom

1 Introduction

The numerical studies of flame acceleration and fast deflagrations in an obstructed channel have been carried out widely over the past ten years [1-4]. Most of these high resolution numerical simulations used a single-step Arrhenius reaction model without explicit turbulent model. So it seems that the turbulence field in the unburned gases ahead of the flame was under-resolved [5]. Johansen and Ciccarelli [5] carried out large eddy simulations of initial flame acceleration using the flame surface density (FSD) combustion model. They showed that the turbulent flame finally enters the “thickened reaction zones” regime during the early stages of the flame acceleration. In this regime, the rate of combustion is more controlled by the rate of chemical reactions than the rate of mixing. Hence, to model the propagation of fast deflagrations in an obstructed channel the artificially thickened flame (ATF) approach [6] which is based on the Arrhenius model seems to be an appropriate option. In this model, it is implicitly assumed that chemistry rather than mixing controls the reaction rate [7]. In this approach, sub-grid scale turbulent mixing is also included using an efficiency function [6]. Another issue about the single step Arrhenius kinetics model is that both flames and detonations cannot be exactly described by the same one-step Arrhenius model, mostly because this model has only a few adjustable parameters. So that, this model may not be appropriate for combustion wave transitions, such as the transition from a laminar to turbulent flame or a turbulent flame to a detonation [3]. Hence, a more complete chemical reaction model is needed. Therefore in this paper the two-dimensional filtered reactive Navier-Stokes equations were solved utilising a chemistry based combustion model (i.e. ATF approach) and using detailed chemical mechanism.

2 Simulation Setup

The basic idea of the ATF approach is to artificially thicken the premixed flame so that the flame front can be resolved on a coarse grid while keeping the laminar flame speed

S_l^0 constant. This is achieved by increasing the molecular diffusion coefficient (D) by a thickening factor (F), whereas the pre-exponential factor of the Arrhenius law (A) is decreased by this factor [8]. Hence, the flame thickness is multiplied by F ($\delta_1^1 = F\delta_1^0$) while the laminar flame speed remains unchanged [8]. The value of the thickening factor F is typically chosen such that the thickened flame structure can be resolved on 10 computational cells (i.e. $\delta_1^1 \cong 10\Delta_x$) [6]. Since the thickened flame is much thicker than the length scales in most parts of the turbulent eddies in the flow, these eddies do not lead to noticeable flame wrinkling. To overcome this drawback, the thickened flame speed is corrected using an efficiency function, E . In fact, the efficiency function can be considered as a sub-grid model to account for the interaction of the flame and turbulence [6]. In the present work, the efficiency function proposed by Colin et al. [6] is used. In the LES/ATF model, the species conservation equation is written as:

$$\frac{\partial(\rho Y_k)}{\partial t} + \frac{\partial(\rho \tilde{u}_j Y_k)}{\partial x_j} = \frac{\partial}{\partial x_j} \left(\rho DEF \frac{\partial Y_k}{\partial x_j} \right) + \frac{\dot{\omega}_k}{F},$$

where u_j , ρ , Y_k and $\dot{\omega}_k$ are the components of the velocity field, density, mass fraction and reaction rate of species k , respectively. The superscript ($\tilde{\cdot}$) denotes a mass-weighted filtered quantity. The same modifications were also implemented for the energy equation.

The LES/ATF model has been applied widely to premixed and partially premixed flames in different configurations with reasonable accuracies (e.g. [9, 10]). Xiao et al. [9] studied a premixed hydrogen/air flame propagation and tulip fame formation in a closed channel using the ATF model and a detailed chemistry. They reported that the flame velocity and pressure during the transient combustion have been well reproduced. Quillatre et al. [10] have shown that using a two-step chemical mechanism, the LES/ATF model accurately reproduce the subsonic flame propagation past repeated obstacles and over-pressure generated in an explosion chamber. In a very recent work of Yu and Navarro-Martinez [11] the effect of thickening procedure on the DDT of shock-flame interaction was studied. They reported that the ATF approach captures the relevant physics and detonation times and lengths are quasi mesh independent [11].

In the present LES simulation, the SGS turbulent viscosity is modeled as a function of the filter size and the SGS turbulent kinetic energy that is described by a transport equation. In addition, a detailed kinetic mechanism was used for stoichiometric hydrogen-air mixture. This mechanism involves 9 species and 27 steps [12]. Also in-situ adaptive tabulation (ISAT) method is also exploited to reduce the computational cost of using detailed chemistry. A second order bounded central scheme is used for diffusion and pressure gradient terms in the governing equations. To avoid numerical dissipation and dispersion a total variation diminishing (TVD) scheme, using the Sweby flux limiter is used for discretization of the convective terms. To treat the pressure–velocity coupling a standard iterative procedure (i.e. PISO algorithm) is employed.

The computational domain is a 2D channel with a length of 64 cm and a width of 4 cm [1, 2] (Fig. 1). The channel is obstructed by rectangular obstacles with a width of $d/16$ and height of $d/4$, where d is the channel width. The first obstacle is placed at a distance of $d/2$ from the closed end and the others are equally spaced at a distance d . The obstacles have blocked half of the channel width, so that the blockage ratio is 0.5.

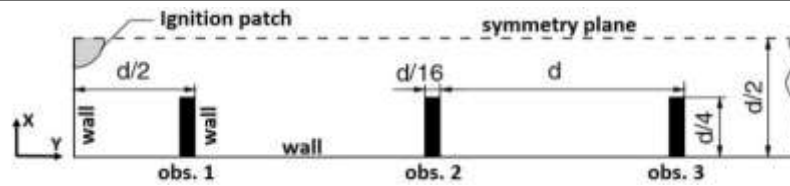


Figure 1. Schematic of the combustion chamber.

3 Verification of the Results

In this section the accuracy of the results in production of the flame speed is verified against the previous studies. In this study a uniformly structured computational grid was used with the cell size of 0.0625 mm. This translates to have 5-6 cells per laminar flame thickness. Furthermore, using a proper artificial thickening factor, the flame front will be resolved here. To verify the present work, a comparison between the present results with those of Gamezo et al. [1] has been shown in Fig. 2. In this figure, the flame tip speed is plotted versus time. A good agreement is observed between the present results with those of Gamezo et al. [1]. It should be pointed out that since the flame acceleration occurs sooner in the numerical experiment of Gamezo et al. [1], for better comparison, the present results are shifted by 0.65 ms. This difference in the onset of acceleration can be attributed to the simple one-step chemistry model used in the work of Gamezo et al. [1]. Because as also commented by Liberman et al. [13] the chemical induction times estimated by the one-step models typically are a few times smaller than the reality. Another source of difference between the current work and that of Gamezo et al. [1] is the difference in calculated laminar burning velocity. This important parameter (especially in the initial time of flame propagation when the flame is laminar) depends on the models used for the calculation of thermo-physical properties, thermo-chemical properties and chemical kinetics. Hence, it is expected that the laminar burning velocity predicted in the present work be different from that of Gamezo et al. [1].

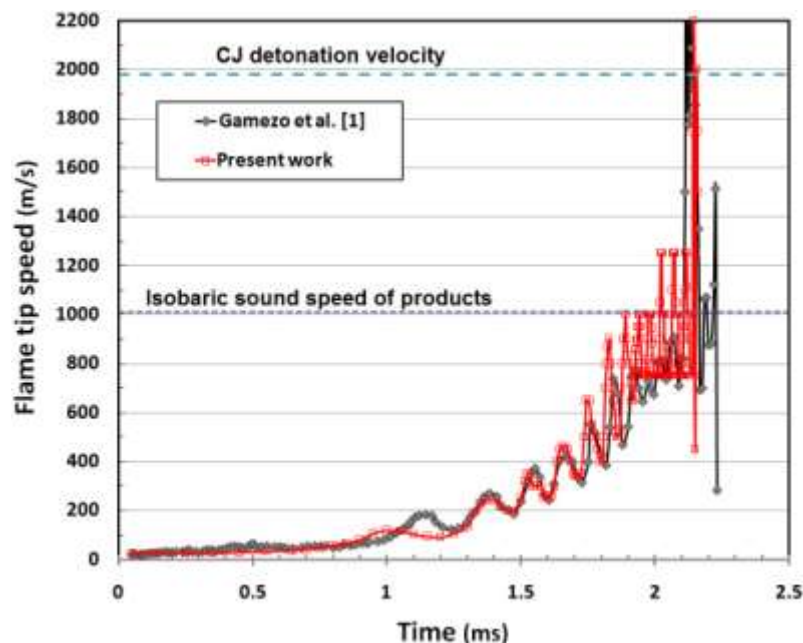


Figure 2. Comparison of the flame tip speed predicted in the present numerical work against the numerical prediction by Gamezo et al. [1].

4 Flame Acceleration and Fast Deflagration

The velocity of the leading edge of the flame front as a function of distance from the ignition point is shown in Fig. 3 (left). Flame acceleration continues until the speed of the flame reaches approximately the isobaric sound speed of the products (i.e., the choked regime). Then, transition from the choked regime to detonation occurs. When the flame passes obstacle No. 6 the flame speed and the velocity of flow at a position ahead of the flame (typically in jet-like flow passing through the obstacles) increases up to the local sound speed of the compressed unburned gas. Consequently, a shock wave is formed in the domain. At this moment, a rapid decline in the flame surface area is observed (Fig. 3 (Right)). In the slow flame regime (before obstacle No. 6) both of the flame surface area and the flame speed increase. In this regime, the interaction of the vortex street ahead of the obstacles with the flame front leads to a considerable flame wrinkling. Hence, the flame acceleration is mainly due to the flame wrinkling [1, 2]. Although, after obstacle No. 6 (where the flame lies in the fast flame regime) the behavior of the flame speed and flame surface area are opposite. It means that the mechanism behind the fast flames propagation differs from the slow flames. When the flame speed reaches the sound speed of the compressed unburned mixture, the flow downstream of the further obstacles is not enhanced and gradually damped. Thus, the strong vortex fields are not formed ahead of the obstacles and as a result extreme wrinkling that was observed in the slow flame propagation regime is not observed at these instants. To describe this discrepancy, the mean rate of energy release, averaged over the flame front is plotted versus the flame location in Fig. 4. In this figure, it is seen that the energy-release rate progressively increases as the flame passes obstacle No. 6. This leads to an increase in the rate of thermal expansion, which causes flame acceleration.

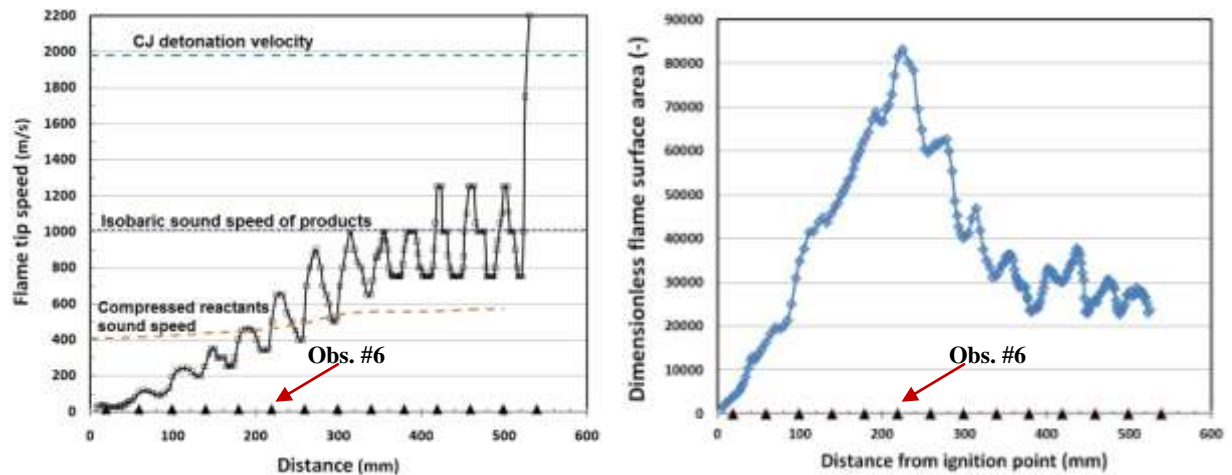


Figure 3. Left: flame tip speed against flame location from the ignition point. Right: dimensionless flame surface area as function of flame tip location. Obstacle locations are signed using triangular symbols.

In Fig. 5, shadowgraph pictures and contours of heat release rate, vorticity magnitude and turbulent velocity fluctuation are plotted on the flame front. In these snapshots it is clearly seen that in the fast flame regime, the interactions between the flame and reflected shocks from the channel walls and obstacles, enhance the amount of heat released [3]. This phenomenon is clearly seen in Fig. 5. In this figure when the flame approaches obstacle No. 11 the interaction of the propagating flame front and the reflected shocks from the obstacles

results in an extreme increase in heat release rate. This is caused by a local increase of temperature and mixing in the flame front by Richtmyer-Meshkov (RM) instability due to the baroclinic vorticity generation mechanism. The present observations are in agreement with the viewpoints of Ciccarelli and colleagues [14] about fast flame propagation mechanism. The present results indicate that in the fast flame regime, the main mechanism responsible for a high level enhancement of flame speed and maintaining the high heat release rate during the flame propagation is shock-flame interactions and the subsequent the RM instability.

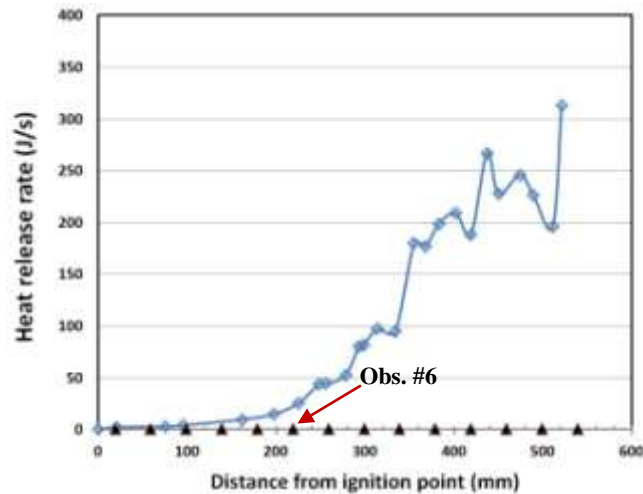


Figure 4. Averaged heat release rate (J/s) over the flame front as function of flame tip location.

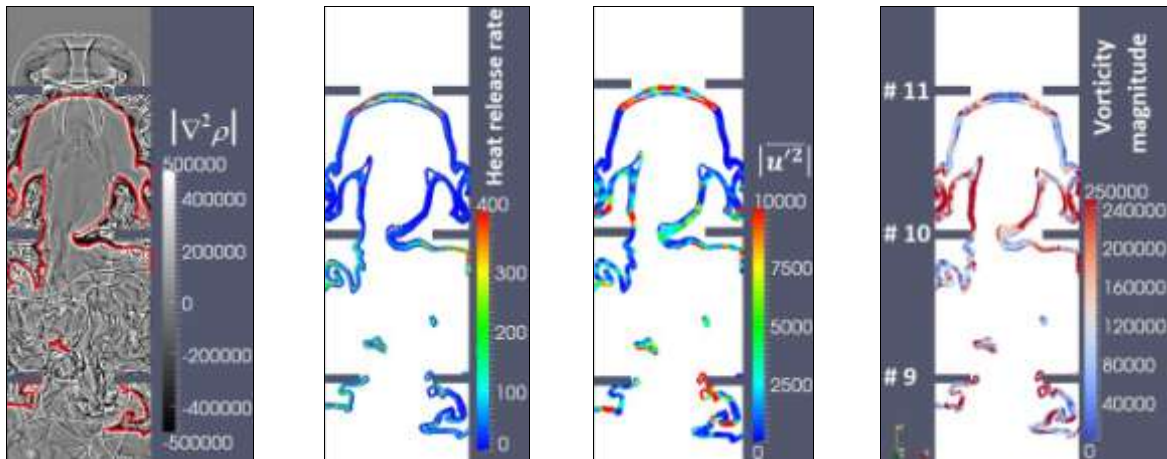


Figure 5. Time sequence of $|\nabla^2\rho|$, heat release rate (J/s), turbulent velocity fluctuations ($|u'^2|$) and vorticity magnitude (1/s) fields respectively from left to right. These parameters have been mapped on the flame front.

5 Conclusions

Using a detailed chemical kinetics, large eddy simulation was performed to examine the flame acceleration and propagation process of fast deflagration in an obstructed channel filled with premixed H₂-Air mixture. The turbulence-chemistry interaction in the SGS scales was

represented using artificially thickened flame approach. To reduce the computational cost imposed by detailed chemical kinetics, the ISAT method was exploited. The results showed that the LES/ATF/ISAT approach qualitatively well reproduces the behavior of a propagating flame during the subsonic and supersonic regimes. It is shown that in the fast flame regime, the flame surface area decreases rapidly, while the flame speed increases toward the choked regime. It is observed that interactions between the flame and the reflected shocks from the channel walls and obstacles, enhance the heat release rate and vorticity generation due to RM instability in the flame front (i.e., the baroclinic mechanism).

References

- [1] Gamezo VN, Ogawa T, Oran ES. (2007). Numerical simulations of flame propagation and DDT in obstructed channels filled with hydrogen–air mixture. *Proc. Combust. Inst.* 31: 2463.
- [2] Gamezo VN, Ogawa T, Oran ES. (2008). Flame acceleration and DDT in channels with obstacles: effect of obstacle spacing. *Combust. Flame.* 155: 302.
- [3] Kessler DA, Gamezo VN, Oran ES. (2010). Simulations of flame acceleration and deflagration-to-detonation transitions in methane-air systems. *Combust. Flame* 157: 2063.
- [4] Heidari A, Wen JX. (2014). Flame acceleration and transition from deflagration to detonation in hydrogen explosion. *Int. J. Hydrog. Energy.* 39: 6184.
- [5] Johansen C, Ciccarelli G. (2013) Modeling the initial flame acceleration in an obstructed channel using large eddy simulation. *J. Loss Prev. Process Indust.* 65: 571.
- [6] Colin O et al. (2000). A thickened flame model for large eddy simulations of turbulent premixed combustion. *Phys. Fluids.* 12: 1843.
- [7] Masri AR, Ibrahim SS, Cadwallader BJ. (2006). Measurements and large eddy simulation of propagating premixed flames. *Experimental Therm. Fluid Science.* 30: 687.
- [8] Butler TD, O’rourke PJ. (1977). A numerical method for two dimensional unsteady reacting flow. *Proc. Combust. Inst.* 16: 1503.
- [9] Xiao H et al. (2013). Dynamics of premixed hydrogen/air flame in a closed combustion vessel. *Int. J. Hydrog. Energy.* 38: 12856.
- [10] Quillatre P, Vermorel O, Poinso T. (2011). Large eddy simulation of turbulent premixed flames propagation in a small scale venting chamber: influence of chemistry and transport modeling. 7th Mediterranean Comb. Symp.: TC-01.
- [11] Yu S, Navarro-Matinez S. (2015). Modelling of deflagration to detonation transition using flame thickening. *Proc. Combust. Inst.* 35:1955.
- [12] Marinov NM, Westbrook CK, Pitz WJ. (1996). Detailed and global chemical kinetics model for hydrogen. In Chan SH, editor, *Transp. Phenom. Combust.* 1:118.
- [13] Liberman MA et al. (2010). Deflagration-to-detonation transition in highly reactive combustible mixtures. *Acta Astronaut.* 67: 688.
- [14] Ciccarelli G, Johansen CT, Parravani M. (2010). The role of shock-flame interactions on flame acceleration in an obstacle laden channel. *Combust. Flame* 157: 2125.